Procedure for the correct placement of Long-Thread Short-Thread couplers in mechanical connections of reinforcing bars

Enrique Hernández-Montes[*1], Fouzia Larbi-Chaht [2a], Mohamed Mouli [2b], Lahouari Mammar [3c],
Sadek Mahdjouba [3], Ahmed M. Mohamed [2], Abdelkader Medjahed [2],
Ahmed Messaoud-Djebara [2] and Luisa María Gil-Martín [1c]

[1] *School of Civil Engineers, University of Granada, Spain*
[2] *Civil Engineering and Environmental Laboratory (LGCE) (UDL of Sidi bel Abess), National Polytechnic School of Oran (ENPO), Algeria*
[3] *Civil Engineering Department, USTOran, Algeria*

Abstract. The present work provides a new solution to both the correct execution and quality control of straight thread couplers for reinforcing bars under monotonic loading conditions. A random survey on already constructed couplers together with a new mechanical model, adjusted with an experimental campaign, led us to present this new procedure in reinforced concrete construction. Formulation and methodology for a correct placement of straight thread couplers is presented.

Keywords: connectors; mechanical splice; reinforcing bars; reinforced concrete construction

1. Introduction

Spliced steel reinforcement in concrete structures (Canbay 2007, Safan 2012 and Sharbatdar *et al*. 2018) may be lapped (Al-Azzawi *et al*. 2020, Turk and Yildirim 2003, Karabinis 2002, and Ma *et al*. 2021) or mechanically connected using different technologies (Kim and Lee 2012, Pimanmas and Thai 2011, and Lu *et al*. 2019).

Mechanical couplers are devices used to connect reinforcing bars in concrete construction. This type of connection provides a less congestive and more reliable splice than lap splicing under cyclic loading conditions. The Concrete Reinforcing Karkarna *et al*. (2020) especially Steel Institute has classified up to sixteen different types of mechanical couplers (CRSI 2020). One of these is the Upset Straight Thread Coupler. This coupler has an internal thread which joins two upset end reinforcing bars. There are several brands and manufacturers whose couplers have different peculiarities that can be classified into this type.

Though some seismic regulations explicitly prohibit couplers in the plastic zones of columns for high seismic regions (e.g., American Association of State Highway and Transportation 2014), several authors (Bompa and Elghazouli 2019, and Tazarv and Saiidi 2016) have checked the good behavior of mechanical couplers when subjected to cyclic loadings. Nevertheless, designers and engineers are reluctant to implement the use of thread couplers due to the lack of guidance for the correct placement and inspection of them.

2. The Long-thread short-thread mechanical coupler

The mechanical coupler denominated long-thread short-thread (hereinafter, LTST-coupler) is a tube with external diameter D, length L and an internal thread, similar to a long nut (see Fig. 1(a)), this coupler can be used as an Upset Straight Thread Coupler. In order to connect two reinforcing bars using a LTST-coupler, a long thread is performed in the extreme-to-connect of one of the reinforcing bars and a short thread is carried out in the extreme-to-connect of the other bar, (see Fig. 1). The mechanical coupler is completely threaded to the long-thread bar, an operation that is usually done at the workshop (see Fig. 1(b)) before transportation to the site. The alignment with the other bar is done at the work site, where the coupler is screwed to the short-threaded bar while being unscrewed from the long-threaded bar. To avoid weakening the reinforcing bar, the end of the bar where the threading is to be carried out is enlarged. During the installation procedure, a torque wrench should not be necessary.

Despite the simplicity of this type of coupler, many users are reluctant to use them due to both the error that can be made during placement and the lack of a standardized control procedure for its use.

This work proposes a precise, simple procedure to ensure the correct installation of this type of coupler. In order to do this, a numeral and experimental campaign and a theoretical analysis have been done. Moreover, a field survey of different construction sites has been conducted.

∗Corresponding author, Professor,
 E-mail: emontes@ugr.es
[a] Assistant Professor,
 E-mail: fouzia.larbi-chaht@enp-oran.dz
[b] Professor, E-mail: moulimohamed@yahoo.fr
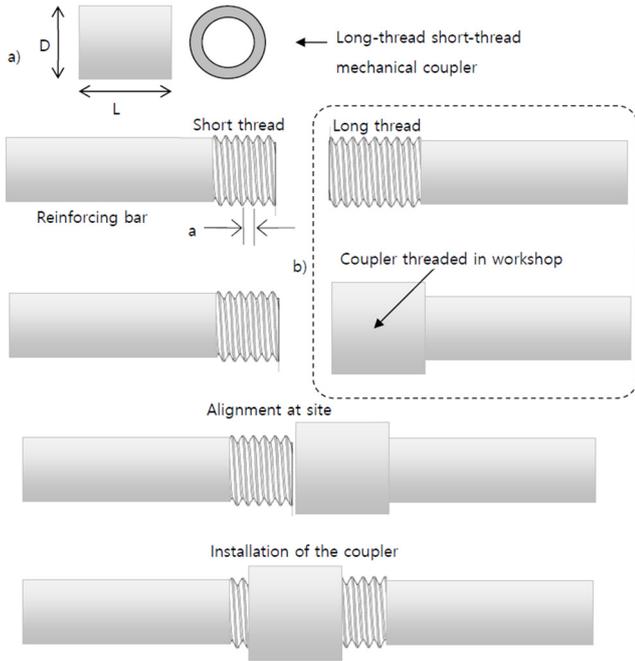[c] Professor, E-mail: mlgil@ugr.es

Fig. 1 Installation of the LTST-coupler

Table 1 Main characteristics of LTST-couplers for Ø16, Ø20, Ø25 and Ø32 bars

Bar diameter (mm)	D (mm)	L (mm)	a (mm)	$n_{theoretical}$
16	25.9	45.5	2.5	2.77
20	31.7	53.9	3.0	2.89
25	41.3	69.9	3.5	3.09
32	50.8	88.9	3.0	4.62

3. Transmission of forces by the threads: the failure surface

Common LTST-couplers available on the market have a coarse thread, mainly due to the fact that their stripping strengths are greater for the same length of engagement and their assembly is quicker. Due to the fact that the capacity of the coupler should be greater than the capacity of the reinforcing bar, the LTST-couplers usually have two modes of failure: failure outside the coupler due to tension in the bar, or failure inside the coupler due to shear collapse in the threaded bar. This last failure mode is also known as stripping failure.

Table 1 shows the D and L dimensions of the couplers analyzed (see Fig. 1(a)) for bars of 16, 20, 25, and 32 mm diameter. The third column shows the pitch of the threaded bar (a) of one of the commercial suppliers, see Fig. 2.

Depending on the width of the contact zone between the coupler and the threaded bar, w (see Fig. 2), the failure surface involved in the stripping failure mode varies from a maximum value to zero, with the real failure surface being the one shown with a dashed red line, see Fig. 2. The maximum failure surface is also depicted in Fig. 2 (dashed black line) and its corresponding force $F_{max, inside}$ is
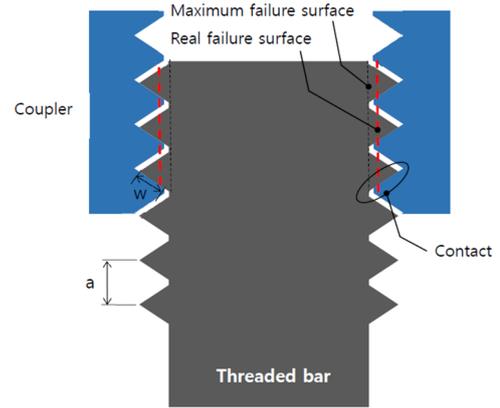

Fig. 2 Failure surfaces in stripping failure

$$F_{max,inside} = \pi \phi a n \tau_{max} \qquad (1)$$

where ϕ is the internal diameter of the thread, which should coincide with the diameter of the bar, a is the pitch of the thread, n is the number of pitches introduced into the coupler and τ_{max} is the shear strength of the steel of the bar. If the contribution of the normal stress on the failure surface is not considered and the Von Mises criterion is applied, $F_{max,inside}$ can be approximated by

$$F_{max,inside} = \pi \phi a n \frac{f_y}{\sqrt{3}} \qquad (2)$$

with f_y as the yield stress of the steel of the bar.

The value of $F_{max,inside}$ corresponds to the maximum value of the contact zone (w), that is, the maximum failure surface shown in Fig. 2. The simplest way to formulate the real value of the stripping force is multiplying Eq. (2) by a factor α

$$F_{inside} = \alpha \pi \phi a n \frac{f_y}{\sqrt{3}} \qquad (3)$$

F_{inside} given by Eq. (3) corresponds to the real failure surface (red dashed line) shown in Fig. 2. Note that, for the same value of n, if the width of the contact zone (w) decreases, then the stripping failure force also decreases.

The resistance of the bar against tension, that is, the outside-mode failure ($F_{outside}$), is given by

$$F_{outside} = \pi \frac{\phi^2}{4} f_y \qquad (4)$$

For the maximum failure surface, the minimum value of n that warranties an outside-mode failure can be obtained by equating Eq. (2) to Eq. (4) and solving for n. The value obtained is called $n_{theoretical}$ and it is shown in the fourth column of Table 1.

$$n_{theoretical} = \frac{\phi \sqrt{3}}{4a} \qquad (5)$$

When considering the real failure surface, the minimum value of n to avoid inside failure is obtained by equating Eq. (3) to Eq. (4) and solving for n. In doing so, the value n_{real} is

Table 2 Laboratory tension tests of couplers

Specimen	n	a (mm)	Ø (mm)	F (kN)	σ_{max} (MPa)	Failure mode	α
Ø16T1-6s	6	2,5	16	132,33	658,15	outside	
Ø16T2-6s	6	2,5	16	137,78	685,25	outside	
Ø16T3-6s	6	2,5	16	131,87	655,9	outside	
Ø16T1-5s	5	2,5	16	137,19	682,31	outside	
Ø16T2-5s	5	2,5	16	138,8	690,36	outside	
Ø16T3-4s	4	2,5	16	124,13	617,36	**inside**	0,658
Ø20T1-5s	5	3	20	203,09	646,46	outside	
Ø20T2-5s	5	3	20	205,5	654,13	outside	
Ø20T3-5s	5	3	20	201,47	641,30	outside	
Ø20T1-4s	4	3	20	205,68	654,71	outside	
Ø20T2-4s	4	3	20	205,22	653,23	outside	
Ø20T3-4s	4	3	20	204,51	650,97	outside	
Ø25T1-5s	5	3,5	25	314	640,8	outside	
Ø25T3-5s	5	3,5	25	318,14	648,1	outside	
Ø25T1-4s	4	3,5	25	314,18	648,18	**inside**	0,761
Ø25T2-4s	4	3,5	25	257,05	523,66	**inside**	0,623
Ø25T3-4s	4	3,5	25	311,95	635,5	**inside**	0,756
Ø32T1-5s	5	3	32	450,38	560	**inside**	0,796
Ø32T2-5s	5	3	32	466,55	580,11	**inside**	0,824
Ø32T3-5s	5	3	32	476,64	592,7	**inside**	0,842
Ø32T1-4s	4	3	32	334,97	416,5	**inside**	0,740
Ø32T2-4s	4	3	32	315,45	392,23	**inside**	0,697
Ø32T3-4s	4	3	32	385,08	478,8	**inside**	0,851

obtained

$$n_{real} = \frac{1}{\alpha} \frac{\phi \sqrt{3}}{4a} \qquad (6)$$

Theoretically, if the bar is driven into the coupler a number of pitches greater than $n_{theoretical}$, then the failure mode should be outside type. Additionally, if the width of the contact zone (w) decreases the number of pitches n needed to warranty an outside type failure will be greater. Based on experimental work, factor α is adjusted in order to formulate the minimum number of pitches (n_{real}) needed for a correct mechanical connection with LTST-couplers.

4. Laboratory experimental campaign

In order to evaluate the number of pitches required for a correct mechanical connection (Eq. (6)), 24 tension tests have been performed (see Table 2). Fig. 3 shows the specimen Ø25T1-4s, failed by stripping, and its corresponding force-deformation curve.

When applying Eq. (3) to the specimens that show stripping failure mode, the parameter α has been calculated, see the final column of Table 2. Additionally, these values have been represented in Fig. 4. As a first approximation, α is considered to be a constant, that is, independent of both the bar size and the pitch distance. The mean value obtained of α is 0.75, and its standard deviation is 0.077. Assuming a normal distribution and a confidence level of 95% for strength design, the corresponding value of α is 0.63. Hence, $\alpha = 0.63$ is going to be adopted.
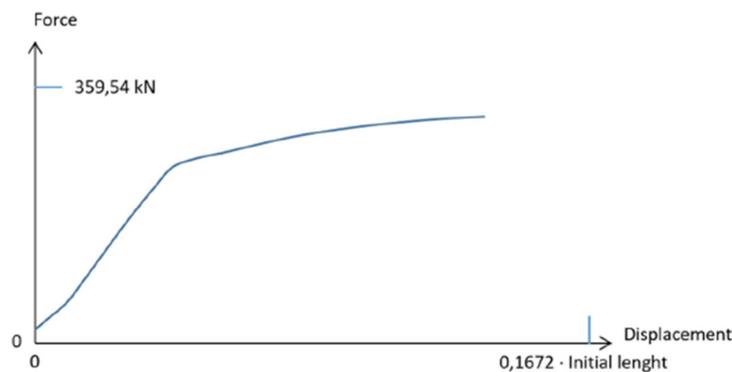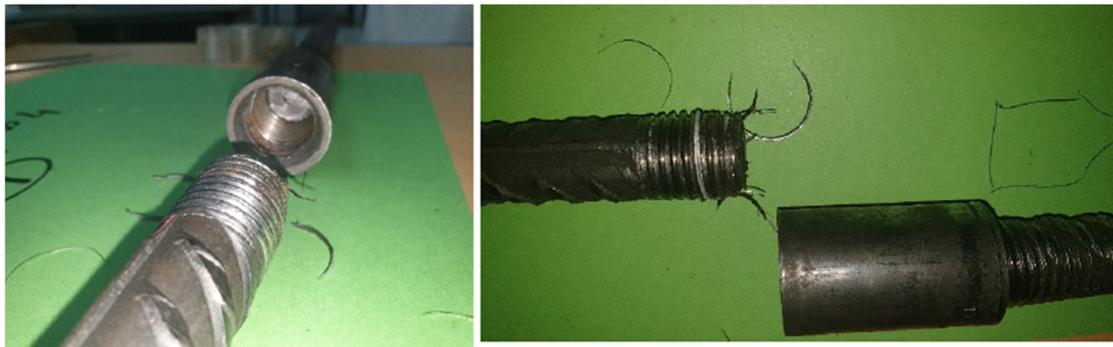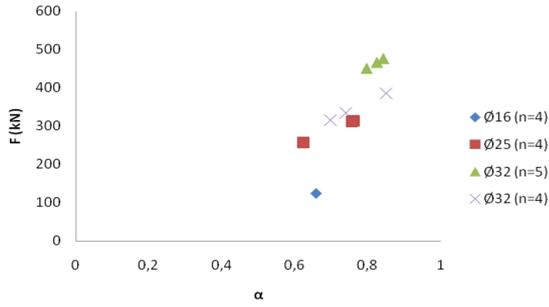

Fig. 3 Specimen Ø25T1-4s

Fig. 4 Values of α for the specimens with stripping failures

A correct mechanical splice using LTST-couplers requires a minimum number of pitches (n_{real} from Eq. (6)). For the specimens shown in Table 1, the value of n_{real} to be used in strength design is shown in Table 3.

Table 3 Strength design value of the number of pitches for Ø16, Ø20, Ø25 and Ø32 bars

Bar diameter (mm)	a (mm)	n_{real}
16	2.5	4.4
20	3.0	4.6
25	3.5	4.9
32	3.0	7.3

5. Survey at site work

Besides the drawbacks arising from placing the connection with a lack of reference, an additional disadvantage of the LTST-couplers is the difficulty of performing reliable inspections once the coupler has been installed. In other words, it is difficult to measure how far the bar has been introduced into the coupler. However, the
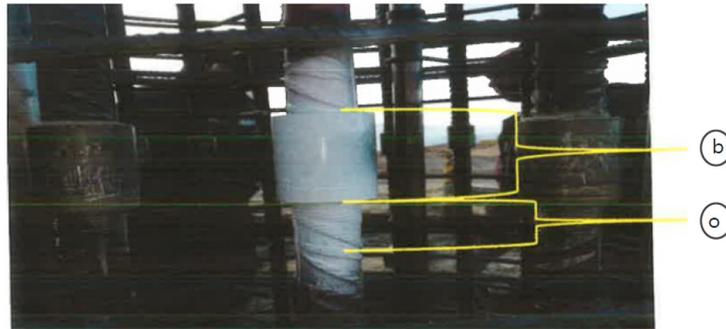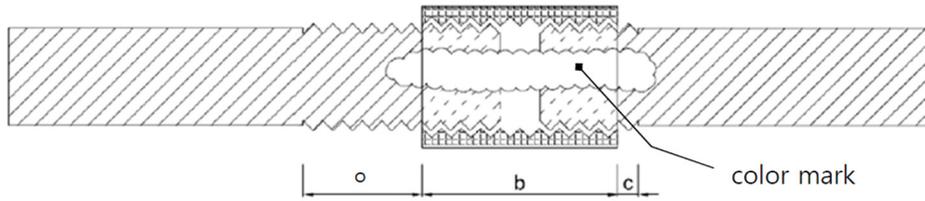
(a)
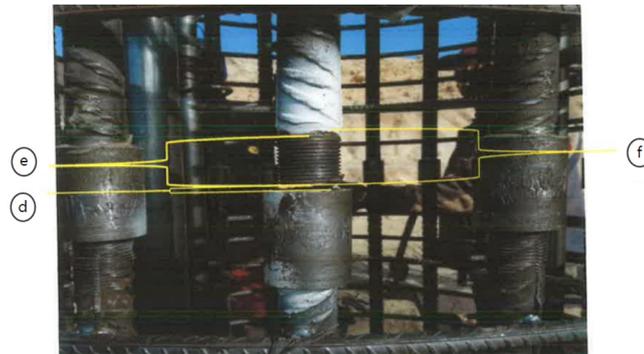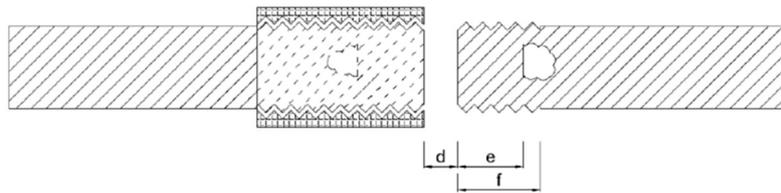
(b)

Fig. 5 Experimental survey

LTST-coupler also has an objective advantage as it is the easiest coupler to install because once the two bars are aligned there is no need to twist any of the bars and only the coupler rotates.

A survey has been conducted at different construction sites in Algeria. A random selection of couplers installed were considered. Distances *o*, *b* and *c* (see Fig. 5(a)) were measured and the connection was later painted in color. After this, the connection was unscrewed (see Fig. 5(b)) and the distances *d*, *e* and *f* were measured.

Based on these measurements, the engagement lengths of each extreme of the bars were calculated, see Table 4. In Table 4, 11 tested specimens have been collected. The value of n in Table 4 represents the number of pitches introduced into each side of each connection (obtained as Length/a). Great variability in the number of pitches introduced into each side of the connection can be observed. Left engagement goes from 8.00 to 14.33 and right engagement goes from 10.67 to 16.33. The reason for this variation is that the worker has no direct knowledge of how well he/she is performing the connection.

A direct comparison between Tables 3 and 4 show that all the connections studied were carried out correctly (note that n > 7.3, see Table 3) although a great dispersion in the number of pitches exists. Note that a larger minimum value (e.g., left side of P18-8 or left side of P27-10) will increase the safety of the connection.

6. Innovation

Providing reinforcing bars with two marks (see Fig. 6) is an innovative procedure that would avoid the variation shown in Table 4, ensuring that proper installation and inspection can be carried out, and, at the same time, saving working time.

The red mark is a reference for the worker. He/She can stop twisting the coupler as soon as the red mark is not visible. The white mark allows for a more detailed

inspection, as values *d* and *e* shown in Fig. 5 can be detduced deduced (see Fig. 7). The white mark should be placed at a constant distance from the end (d_{white}). The distances im_1 and im_2 can be measured during a detailed inspection, and the distance of each bar inserted into the coupler (e_1 and e_2) and the existing gap (*d*) can be calculated.

$$e_1 = d_{white} - im_1$$
$$e_2 = d_{white} - im_2 \qquad (7)$$
$$d = L - e_1 - e_2$$

7. Conclusions

The present work is extremely useful for overcoming the reluctance to use of LTST (long-thread short-thread) mechanical couplers for the splicing of reinforcing bars at work sites. Supported by both a survey at different work sites and an experimental campaign, a theoretical development and a practical implementation have been presented which allows the correct execution and inspection of this type of connection.

Table 4 Engagement length and equivalent number of pitches of connections studied in the survey (ϕ = 32 mm, b = 80 mm, a = 3.0 mm –see Fig. 5-)

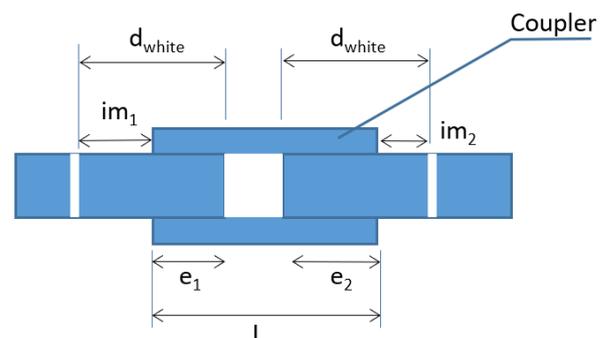| Denomination	Left engagement		Right engagement	
	Length (mm)	n	Length (mm)	n
P5-P10	33	11.0	45	15.00
P6-P8	40	13.33	32	10.67
P13-P10	32	10.67	42	14.00
P15-P10	37	12.33	40	13.33
P16-P10	32	10.67	39	13.00
P18-P8	24	8.00	43	14.33
P21-P10	40	13.33	34	11.33
P22-P10	32	10.67	44	14.67
P23-P10	43	14.33	34	11.33
P24-P10	40	13.33	35,9	11.97
P27-P10	29	9.67	49	16.33

Fig. 6 Marked reinforcing bar

Fig. 7 Detailed inspection

Acknowledgments

References

Al-Azzawi, A.A., Daud, R.A. and Daud, S.A. (2020), "Behavior of tension lap spliced sustainable concrete flexural members", *Adv. Concrete Constr., Int. J.*, **9**(1), 83-92. https://doi.org/10.12989/acc.2020.9.1.083

American Association of State Highway and Transportation (2014), AASHTO Guide Specifications for LRFD Seismic Bridge Design, Washington, D.C., USA.

Bompa, D.V. and Elghazouli, A.Y. (2019), "Inelastic cyclic behaviour of RC members incorporating threaded reinforcement couplers", *Eng. Struct.*, **180**, 468-483. https://doi.org/10.1016/j.engstruct.2018.11.053

Canbay, E. (2007), "Comparison of code provisions on lap splices", *Struct. Eng. Mech., Int. J.*, **27**(1), 63-75. https://doi.org/10.12989/sem.2007.27.1.063

CRSI (2020), Concrete Reinforcing Steel Institute; Splicing Bar.

Karabinis, A.I. (2002), "Reinforced concrete beam-column joints with lap splices under cyclic loading", *Struct. Eng. Mech., Int. J.*, **14**(6), 649-660. https://doi.org/10.12989/sem.2002.14.6.649

Karkarna, Y.M., Bahadori-Jahromi, A., Jahromi, H., Halliwell, E. and Goodchild, C. (2020), "Comparative study of factors influencing tension lap splices in reinforced concrete beams", *Adv. Concrete Constr., Int. J.*, **10**(4), 279-287. https://doi.org/10.12989/acc.2020.10.4.279

Kim, H.K. and Lee, S.H. (2012), "Lateral confining action of mortar-filled sleeve reinforcement splice", *Struct. Eng. Mech., Int. J.*, **41**(3), 379-393. https://doi.org/10.12989/sem.2012.41.3.379

Lu, Z., Huang, J., Li, Y., Dai, S., Peng, Z., Liu, X. and Zhang, M. (2019), "Mechanical behaviour of grouted sleeve splice under uniaxial tensile loading", *Eng. Struct.*, **186**, 421-435. https://doi.org/10.1016/j.engstruct.2019.02.033

Ma, F., Deng, M., Ma, Y., Lü, H., Yang, Y. and Sun, H. (2021), "Experimental study on interior precast concrete beam–column connections with lap-spliced steel bars in field-cast RPC", *Eng. Struct.*, **228**, 111481. https://doi.org/10.1016/j.engstruct.2020.111481

Pimanmas, A. and Thai, D.X. (2011), "Response of lap splice of reinforcing bars confined by FRP wrapping: application to nonlinear analysis of RC column", *Struct. Eng. Mech., Int. J.*, **37**(1), 111-129. https://doi.org/10.12989/sem.2011.37.1.111

Safan, M.A. (2012), "Behaviour of fiber reinforced concrete beams with spliced tension steel reinforcement", *Struct. Eng. Mech., Int. J.*, **43**(5), 623-636. https://doi.org/10.12989/sem.2012.43.5.623

Sharbatdar, M.K., Jafari, O.M. and Karimi, M.S. (2018), "Experimental evaluation of splicing of longitudinal bars with forging welding in flexural reinforced concrete beams", *Adv. Concrete Constr., Int. J.*, **6**(5), 509-525.
https://doi.org/10.12989/acc.2018.6.5.509

Tazarv, M. and Saiidi, M.S. (2016), "Seismic design of bridge columns incorporating mechanical bar splices in plastic hinge regions", *Eng. Struct.*, **124**, 507-520. https://doi.org/10.1016/j.engstruct.2016.06.041

Turk, K. and Yildirim, M.S. (2003), "Bond strength of reinforcement in splices in beams", *Struct. Eng. Mech., Int. J.*, **16**(4), 469-478. https://doi.org/10.12989/sem.2003.16.4.469

CC